Author(s): Rubert, J.; Dorvaux, Olivier; Gall, Benoit; Greenlees, Paul; Asfari, Z.; Piot, J.; Andersson, L.; Asai, M.; Cox, D.M.; Dechery, F.; Grahn, Tuomas; Hauschild, Karl; Henning, G.; Herzan, Andrej; Herzberg, Rolf-Dietmar; Hessberger, Fritz Peter; Jakobsson, Ulrika; Jones, Peter; Julin, Rauno; Juutinen, Sakari; Ketelhut, Steffen; Khoo, T-L; Leino, Matti; Ljungvall, J.; Lopez-Martens, Araceli; Lozeva, R.; Nieminen, Päivi; Pakarinen, Janne; Papadakis, Philippos; Parr, E.; Peura, Pauli; Rahkila, Panu; Rinta-Antila, Sami;

Title: First prompt in-beam gamma-ray spectroscopy of a superheavy element: the 256Rf

Year: 2013

Version:

Please cite the original version:

Rubert, J., Dorvaux, O., Gall, B., Greenlees, P., Asfari, Z., Piot, J., Andersson, L., Asai, M., Cox, D.M., Dechery, F., Grahn, T., Hauschild, K., Henning, G., Herzan, A., Herzberg, R.-D., Hessberger, F. P., Jakobsson, U., Jones, P., Julin, R., . . . Venhart, M. (2013). First prompt in-beam gamma-ray spectroscopy of a superheavy element: the 256Rf. In 11th International Conference on Nucleus-Nucleus Collisions (NN2012), 27 May to 1 June 2012, San Antonio, Texas, USA (Article 012010). Institute of Physics. Journal of Physics: Conference Series, 420. https://doi.org/10.1088/1742-6596/420/1/012010

First prompt in-beam γ-ray spectroscopy of a superheavy element: the ^{256}Rf

2013 J. Phys.: Conf. Ser. 420 012010

(http://iopscience.iop.org/1742-6596/420/1/012010)

Journal of Physics: Conference Series **420** (2013) 012010 doi:10.1088/1742-6596/420/1/012010

First prompt in-beam γ-ray spectroscopy of a superheavy element: the ^{256}Rf

J. Rubert[1], O. Dorvaux[1], B.J.P. Gall[1], P.T. Greenlees[2], Z. Asfari[1], J. Piot[1,*], L.L. Andersson[3], M. Asai[4], D.M. Cox[3], F. Dechery[5], T. Grahn[2], K. Hauschild[6], G. Henning[6,7], A. Herzan[2], R.-D. Herzberg[3], F.P. Heßberger[8], U. Jakobsson[2], P. Jones[2], R. Julin[2], S. Juutinen[2], S. Ketelhut[2], T.-L. Khoo[7], M. Leino[2], J. Ljungvall[6], A. Lopez-Martens[6], R. Lozeva[1], P. Nieminen[2], J. Pakarinen[9], P. Papadakis[3], E. Parr[3], P. Peura[2], P. Rahkila[2], S. Rinta-Antila[2], P. Ruotsalainen[2], M. Sandzelius[2], J. Sarén[2], C. Scholey[2], D. Seweryniak[7], J. Sorri[2], B. Sulignano[5], Ch. Theisen[5], J. Uusitalo[2] and M. Venhart[10]

[1] Institut Pluridisciplinaire Hubert Curien, Université de Strasbourg, 23 rue du Loess F-67037 Strasbourg, France
[2] Department of Physics, University of Jyväskylä, FIN-40014 Jyväskylä, Finland
[3] Department of Physics, University of Liverpool, Oxford Street, Liverpool, L69 7ZE, UK
[4] Advanced Science Research Center, Japan Atomic Energy Agency, Tokai, Ibaraki 319-1195, Japan
[5] CEA, Centre de Saclay, IRFU/Service de Physique Nucléaire, F-91191 Gif-sur-Yvette, France
[6] CSNSM, IN2P3-CNRS, F-91405 Orsay Campus, France
[7] Argonne National Laboratory, Argonne, Illinois, Illinois 60439, USA
[8] GSI, Helmholzzentrum für Schwerionenforschung GmbH, Planckstr. 1, 64291 Darmstadt, Germany
[9] CERN-ISOLDE, Building 26, 1-013, CH-1211 Geneva 23, Switzerland
[10] Institute of Physics, Slovak Academy of Sciences, SK-84511 Bratislava, Slovakia
[*] Present address: GANIL, CEA/DSM-CNRS/IN2P3, Caen, France

E-mail: `jerome.rubert@iphc.cnrs.fr`

Abstract. Using state-of-the-art γ-ray spectroscopic techniques, the first rotational band of a superheavy element, extending up to a spin of 20 $\hbar$, was discovered in the nucleus ^{256}Rf. To perform such an experiment at the limits of the present instrumentation, several developments were needed. The most important of these developments was of an intense isotopically enriched ^{50}Ti beam using the MIVOC method. The experimental set-up and subsequent analysis allowed the ^{256}Rf ground-state band to be revealed. The rotational properties of the band are discussed and compared with neighboring transfermium nuclei through the study of their moments of inertia. These data suggest that there is no evidence of a significant deformed shell gap at $Z = 104$.

1. Introduction

The definition of the proton number forming the low-Z border to the superheavy element (SHE) region is often a subject of discussion. A superheavy element can be defined as an element with a

macroscopic fission barrier calculated within the liquid drop model which leads to lifetimes lower than the time needed to form a compound nucleus or a molecule such as hydrogen. Superheavy elements only exist thanks to the nuclear shell and pairing effects, which give enhanced stability and result in finite lifetime. Therefore, $Z = 104$ is often defined as border of superheavy elements. Furthermore, the half-life systematics of even-even heavy nuclei presented in Ref. [1] shows that starting from rutherfordium isotopes ($Z = 104$), gaps at larger neutron numbers start to play significant role.

In the quest to discover the heaviest elements, the existence of a new element is usually established on the basis of the observation of their α decay chain and fission properties. Therefore, only a very limited number of excited states populated are observed with rather low statistics. At the lowest border of this SHE region, cross sections are below the limits of observation for state-of-the-art instrumentation employed in decay-tagged prompt γ-ray spectroscopy. In the transfermium region, detailed spectroscopic studies have been performed in many nuclei around ^{254}No in recent years. The growing number of experimental results allowed systematic studies of the location and evolution of single-particle states. The study of K-isomers and associated rotational band structures, and in-beam prompt γ-ray spectroscopy are two major ways to investigate these structures.

Thanks to efficient tagging techniques, in-beam experiments were performed in the transfermium region up to ^{255}Lr ($Z = 103$). Reviews of the experimental results in this field are available in Refs. [2, 3]. Experimental data on rotational bands and associated moments of inertia can be compared to theoretical predictions in order to gain knowledge on the orbitals near their Fermi surface. Great hope is placed in gaining confidence in the theoretical extrapolations of the position of the long-sought Island of Stability [4].

In a recent experiment dedicated to prompt spectroscopy of ^{246}Fm [5], the observational limits were pushed down to the level of 11 nb, opening the way to the spectroscopy of a superheavy nucleus, ^{256}Rf. The production cross section in this case is around 16 nb according to [6]. The present proceedings focuses on the recoil-decay-tagged prompt γ-ray study of this nucleus, which allowed the structure of a superheavy nucleus to be explored for the first time. The ^{256}Rf nucleus is of specific interest in this region since it is situated at the neutron deformed shell gap $N = 152$ (as is ^{254}No) and it allows the investigation of a possible proton shell gap at $Z = 104$.

To be able to perform prompt γ-ray spectroscopy of ^{256}Rf at the University of Jyväskylä, Finland, many years of development were necessary to fulfil the four main requirements:

- A lead target that can sustain a beam intensity of up to 70 particle nanoAmps (pnA). A rotating target designed and built at IPHC Strasbourg has been used for several years at the University of Jyväskylä.
- Electronics that can sustain a high counting rate induced in the germanium detectors around target. The JUROGAM II γ-ray detector array was first fully digital-instrumented with TNT2-D cards [7, 8] developed at IPHC Strasbourg and finally with Lyrtech cards adapted by the Daresbury Laboratory and the University of Liverpool.
- High γ-ray detection efficiency of the germanium detector array. The current JUROGAM II array reaches an absolute efficiency of 5.2 % at 1.33 MeV.
- Intense isotopically enriched ^{50}Ti beam. This last achieved requirement was developed at the IPHC and first tested at the University of Jyväskylä [9].

Thanks to all these developments, the ^{256}Rf nuclei could be produced using the "triple-magic" ^{208}Pb(^{50}Ti, 2n) fusion-evaporation reaction and studied with state-of-the-art instrumentation. The high quality of the data acquisition [10] and analysis software [11] allowed the ^{256}Rf rotational band to be revealed online. The preliminary spectrum was already presented while the experiment was still running [12]. The full statistics of the experiment were then carefully analyzed and the results were first published in Ref. [13].

In the next section, the development of the ^{50}Ti beam is presented. The subsequent sections are devoted to the description of the experimental setup and the conditions used in order to identify the ^{256}Rf nuclei. Thereafter, a section is dedicated to the observation of the prompt γ-ray spectrum and followed by a discussion of the spin assignment, and a comparison of the rotational properties with selected transfermium nuclei. Finally, some information concerning known isomers in this nucleus [14, 15] is discussed in the light of these new data.

2. Isotopically enriched ^{50}Ti beam development

Several methods enable the production of an intense isotopically enriched ^{50}Ti beam. After a comparison between all the possible methods at the University of Jyväskylä ECRIS2 ion source [16], the Metal Ions from Volatile Compounds (MIVOC) method was chosen for its quite low material consumption and rather simple use. With this method, the beam is produced by dissociation in the ECR plasma of a volatile organometallic compound. The greatest difficulty in this case is related to the chemistry of the molecule. Suitable MIVOC compounds are characterized by a good chemical stability associated with sufficiently high vapor pressure. More details concerning this method can be found in Ref. [17]. A titanium compound was already tested some years ago [18] but could not supply enough beam intensity due to the rather low proportion of ^{50}Ti (5.18 %) in natural titanium. In order to resolve the issue, it was necessary to synthesize the compound starting from enriched ^{50}Ti material.

During the development and testing phase, several organometallic compounds were tested using a residual gas analyzer at the University of Jyväskylä. Those with sufficiently high vapor pressure were then tested directly in the ECR ion sources. From all the compounds reviewed only two were compatible with MIVOC beam production: the dimethyl-bis-cyclopentadienyl-titanium ($Cp_2Ti(CH_3)_2$) and the trimethyl-pentamethyl-cyclopentadienyl-titanium ($Cp^*Ti(CH_3)_3$), where Cp corresponds to η^5-C_5H_5 and Cp* corresponds to η^5-$C_5(CH_3)_5$. Fig. 1 shows the residual gas analyzer mass spectrum of both of these compounds. One can observe peaks corresponding to several fragments of the MIVOC compound generated by the filament of the mass analyzer. The vapor pressures of the two compounds were quite similar. Since the $Cp_2Ti(CH_3)_2$ was proven to be unstable under high vacuum, the $Cp^*Ti(CH_3)_3$ was selected due to its better behavior, despite its sensitivity to light, air and moisture.

After the successful tests with the natural titanium compound, commercially available $TiCl_4$ enriched to 92% in ^{50}Ti was used as the starting point for synthesis at IPHC Strasbourg. The

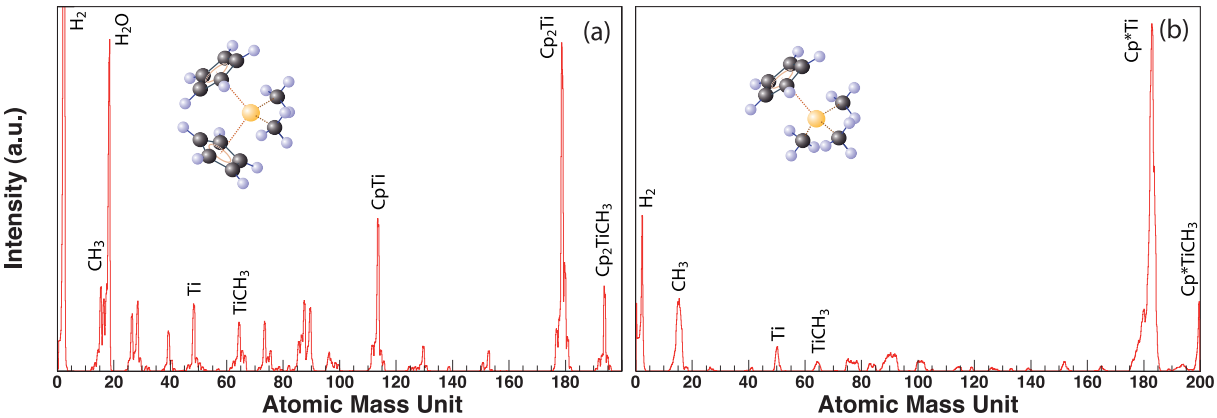

Figure 1. Residual gas analyzer spectrum from: (a) the natural $Cp_2Ti(CH_3)_2$ and (b) the enriched $Cp^*{}^{50}Ti(CH_3)_3$ compounds. Insets: 3D view of the molecules.

corresponding mass spectrum is shown in Fig. 1.b. Intensity of 19 eμA for $^{50}Ti^{11+}$ beam was obtained from the ECRIS2 ion source [9] and accelerated through the K = 130 MeV cyclotron. This beam was then used for the ^{256}Rf experiment which lasted for a total beam-on-target time of 450 hours. The average beam intensity was 29 pnA and reached a maximal value of 45 pnA on target. Quite stable operating conditions were observed during the experiment and a consumption rate of 0.63 mg.h^{-1} was determined. More details of the beam development can be found in Ref. [9].
This compound was later tested successfully in its natural form at two other international laboratories, FLNR (Dubna, Russia) and GANIL (Caen, France). At the University of Jyväskylä, improvements were made to diminish the consumption rate to 0.20 mg.h^{-1} and enhance available beam intensity.

3. Experimental set-up

The experiment was carried out at the Accelerator Laboratory of the University of Jyväskylä, Finland. The $^{50}Ti^{11+}$ beam was accelerated to an energy of 242 MeV to maximize the production cross section with a mid-target beam energy of ≈239 MeV (see Ref. [6]). The beam irradiated a self-supporting ^{208}Pb target with a thickness of 446 μg/cm^2 which was rotated in order to avoid deterioration under radiation.
The experimental set-up was composed (from upstream to downstream) of the JUROGAM II Ge array, the RITU gas-filled separator [19] and the GREAT focal-plane detection system [20]. Prompt γ-rays emitted at the target were detected by the germanium detector array. JUROGAM II was composed of 15 tapered and 24 clover Compton-suppressed high-purity Ge detectors. The measured absolute detection efficiency was 5.2 % at 1.33 MeV, when using the add-back method for the clover detectors. All JUROGAM II Ge detectors were instrumented with Lyrtech VHS-ADC digital cards.
Using the gas-filled separator RITU, recoiling nuclei were separated from target-like and transfer products by their magnetic rigidity. At the focal plane of RITU, reaction products passed through a Multi-Wire Proportional Counter (MWPC) where the energy loss of the particle was recorded (noted ΔE). Then, they were implanted into two Double-sided Silicon Strip Detectors (DSSDs) of the GREAT detection system, which are placed side-by-side. Time-of-Flight (ToF) was measured as the time difference between the MWPC signal and the implantation in the DSSDs. Each DSSD had a thickness of 300 μm and was divided into 60×40 strips of 1 mm width, defining 2400 pixels of 1 mm^2 per DSSD. The amplifier gains of each side of the DSSDs were set for different purposes: the X-side (horizontal strips) had a range of 2 MeV for conversion electron detection (to search for possible isomeric states) and the Y-side (vertical strips) was tuned to detect recoils and fission energy depositions (up to 250 MeV). Furthermore, a planar germanium detector of thickness 1.5 cm was situated behind the DSSDs in the vacuum chamber, and three clover detectors surrounding the focal plane were added to perform delayed γ-ray spectroscopy.
During the experiment, the energy of every event in all detectors was timestamped by an universal 100 MHz clock and saved using the triggerless Total Data Readout (TDR) method (see Ref. [10]). The correlations between groups of detectors were exploited with the GRAIN data analysis package (see Ref. [11]).

4. ^{256}Rf nuclei identification

Since ^{256}Rf nuclei decay almost exclusively by spontaneous fission (more than 99.5 % according to Ref. [21]), the identification of these nuclei of interest was realized through a selection using the "Recoil-Fission Tagging" technique, a specific version of the usual "Recoil-Decay Tagging" technique. The following conditions were imposed to achieve the selection:

- A recoil implantation and a spontaneous fission event had to be detected successively in the same pixel of the DSSDs.
- The fission energy deposition had to be higher than 25 MeV, in order to avoid selection of electrons, alpha particles, target-like or transfer products. The corresponding energy spectrum is shown in Fig. 2.a.
- The search time between the implantation and the fission event was limited to an optimal value of 100 ms. Fig. 2.b shows the time difference distribution with a logarithmic time scale.
- Recoiling products were selected using an E-ToF matrix, where E is the implantation energy of the recoil in the DSSDs. The corresponding matrix is shown without any selection criteria on Fig. 3.a. It clearly appears that the identification of fusion products is not trivial. However, by imposing a selection with a recoil temporally followed by a fission event in the same pixel, it is possible to make a very clean selection (see Fig. 3.b). The final region used to select fusion products is displayed in red.

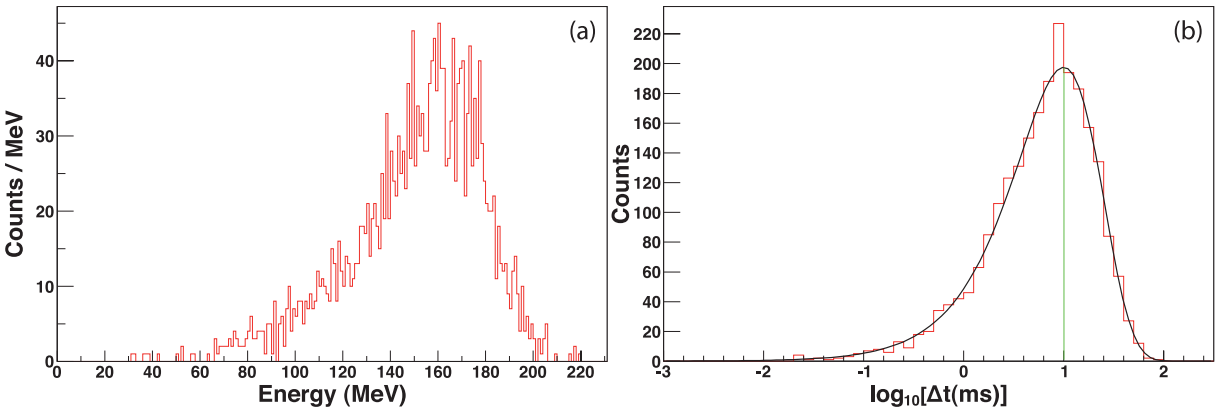

Figure 2. (a) Energy spectrum of correlated fission events detected within 100 ms at the same position in the DSSDs as the implanted recoil. (b) Time difference between correlated recoil and fission events with a logarithmic scale. The green line points the maximum of the curve which corresponds to the value of the ^{256}Rf ground-state life-time.

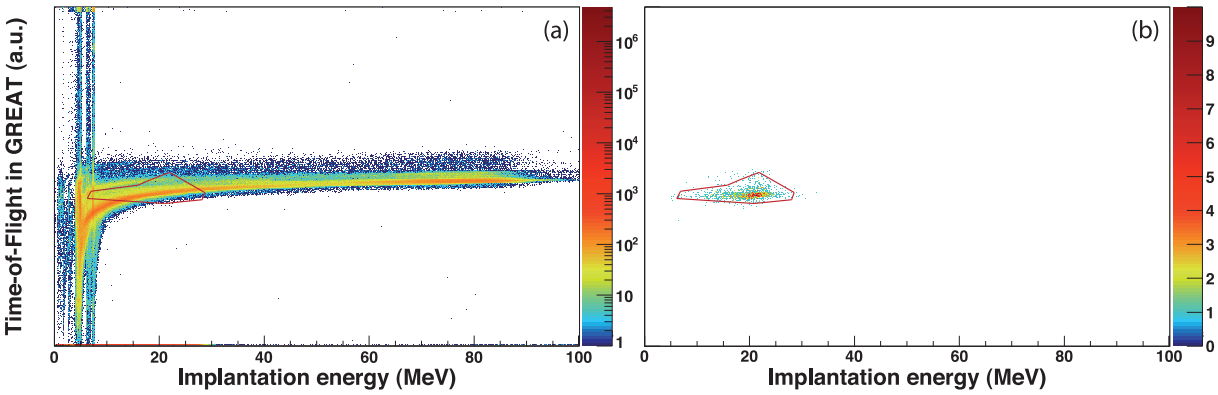

Figure 3. Time-of-Flight in GREAT versus implantation energy matrices for: (a) all recoiling products and (b) recoiling products followed by a fission event. The polygonal gate displayed in red was used for the selection of the correlated events.

This selection allowed unambiguous identification of 2210 correlated events in the duration of the experiment out of more than 10^7 recoiling nuclei implanted in GREAT. Assuming a separator transmission efficiency of 40 ± 5%, a cross section of 17 ± 3 nb was estimated. From the maximum of the curve on Fig. 2.b corresponding to the life-time, one can measure a life-time of 10.0 ms represented by a green line. Therefore, the recoil-fission time difference provided a measured half-life of 6.9 ± 0.2 ms for the ground-state of ^{256}Rf. These two experimental values are consistent with previous measurements as shown in Table 1.

Table 1. Comparison of measured ^{256}Rf spontaneous fission half-lives and production cross section.

Reference	[21]	[6]	[14]	[15]	This work
T_{SF} (ms)	6.2 ± 0.2	6.70 ± 0.09	6.67 ± 0.09	6.9 ± 0.4	6.9 ± 0.2
σ (nb)	12 ± 1	15.7 ± 0.2	17 ± 2	≈14	17 ± 3

5. Prompt γ-ray spectrum

To obtain a prompt γ-ray spectrum associated with the correlated ^{256}Rf decays, a matrix of the recoil Time-of-Flight (in GREAT) versus the time difference between the detection of the γ-rays and the corresponding recoil implantation (basically the Time-of-Flight in RITU) was used (see Fig. 4.a). A two-dimensional polygonal gate (in red on the figure) is displayed around the points that correspond to γ-rays emitted from ^{256}Rf and detected in JUROGAM II. The other points correspond to random coincidences.

This specific selection led to the γ-ray spectrum displayed in Fig. 4.b. One can note the power of selectivity: 745 counts are plotted in the energy range shown, whilst it is estimated that more than 10^{12} γ-rays were detected at the target in the course of the experiment. At low energy, intense peaks due to Pb and Rf X-rays can be observed. A regularly-spaced sequence of eight peaks are labeled with their energies in the figure. The sequence is clearly characteristic of a rotational band, as observed in other transfermium nuclei. The measured transition energies

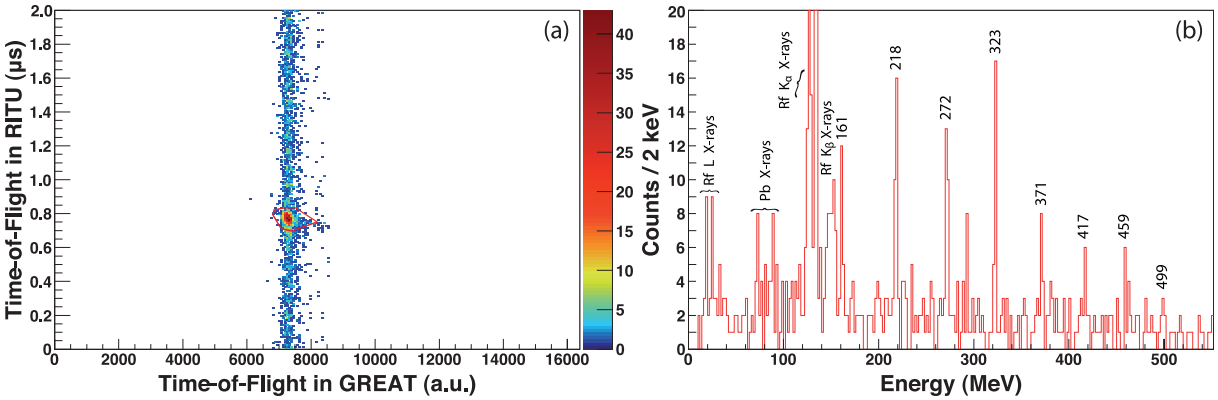

Figure 4. (a) Matrix of the Time-of-Flight in GREAT versus the Time-of-Flight in RITU. The polygonal gate used for the selection of correlated prompt γ-rays is displayed in red. (b) Energy spectrum of prompt singles γ-rays correlated with fission-tagged ^{256}Rf nuclei.

are 161, 218, 272, 323, 371, 417, 459 and 499 keV. The transitions are assigned to the rotational band built on the ground state of ^{256}Rf, showing that this nucleus is deformed.

6. Spin assignment

To assign spins to the observed states, moments of inertia could be obtained according to the formalism of Harris [22]. It is possible to parameterize the rotational band in terms of the kinematic ($\mathcal{J}^1$) and dynamic ($\mathcal{J}^2$) moments of inertia using the following formula:

$$\mathcal{J}^{(1)} = \mathcal{J}_0 + \mathcal{J}_1\omega^2 \tag{1}$$

$$\mathcal{J}^{(2)} = \mathcal{J}_0 + 3\ \mathcal{J}_1\omega^2 \tag{2}$$

where ω is the rotational frequency ($\omega = \mathrm{E}_\gamma/2\hbar$). By fitting the experimental kinematic moment of inertia (calculated with the formula $\mathcal{J}^{(1)} = [I - 1/2]/\omega(I)$, spin values can be assigned to the observed states. Since the nucleus of interest has an even number of protons and neutrons, all spins are supposed to have positive even values. Values of initial spin proposed for the first observed transition (161 keV) were tested against the experimental points using Eq. (1). A reduced χ^2 comparison of these fits is shown on Fig. 5.a where a clear minimum at 6^+ leads to the conclusion that the 161 keV peak corresponds to the transition between the 6^+ and 4^+ states. The spins of the observed rotational structure can then be assigned up to a spin of 20 $\hbar$. Simultaneously, one can extract the two Harris parameters from the corresponding kinematic moment of inertia $\mathcal{J}_0 = 66.7\ \ \hbar^2.\mathrm{MeV}^{-1}$ and $\mathcal{J}_1 = 175.5\ \ \hbar^4.\mathrm{MeV}^{-3}$.

The two lowest transitions cannot be observed due to the dominance of internal conversion for such a high Z nucleus. Using the two above-mentioned parameters, it is possible to extrapolate the energies of the two unobserved transitions 4^+ to 2^+ and 2^+ to 0^+ using the formula:

$$I = \mathcal{J}_0\omega + \mathcal{J}_1\omega^3 + 1/2 \tag{3}$$

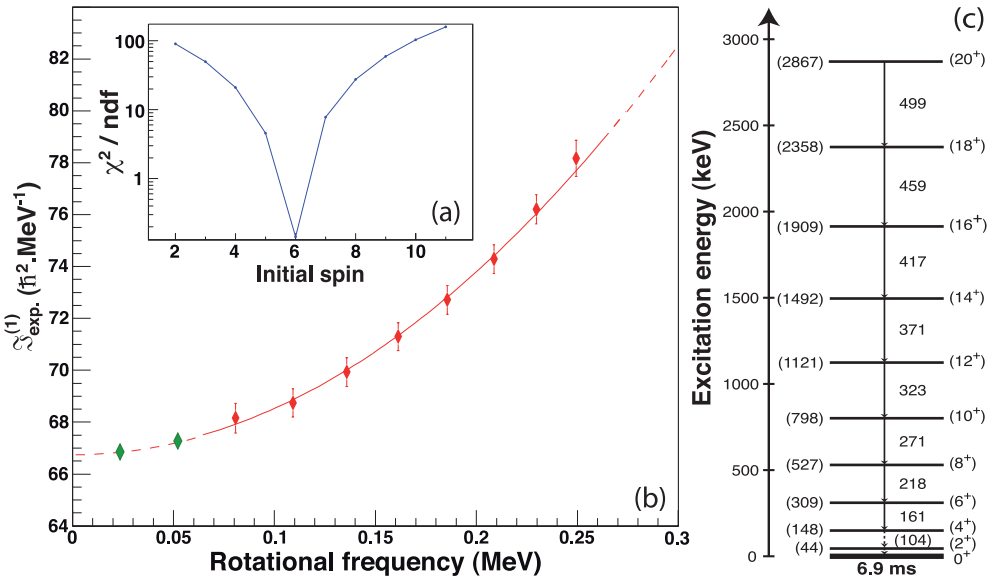

Figure 5. (a) Reduced χ^2 of the Harris fit to the experimental kinematic moment of inertia as a function of the initial spin of the first observed transition. (b) Experimental kinematic moment of inertia for the observed rotational band. Extrapolation of the Harris fit at low energy allows the energies of the two unobserved transitions to be obtained (green dots). (c) Proposed energy level scheme of the rotational band based on the ground state of ^{256}Rf.

where I is the initial spin of the transition [22]. The extrapolation is shown on Fig. 5.b. where the green dots correspond to spins of 4^+ and 2^+. The energies thus obtained are 104 and 44 keV, respectively.
This analysis allows an energy level scheme of the rotational band based on the ^{256}Rf ground state to be proposed, as presented in Fig. 5.c. Full details of the transition energies, spin assignments and relative intensities corrected for detection efficiency and internal conversion are listed in Table 2.

Table 2. List of measured energies and proposed transition assignment of the rotational band, the two first transitions are extrapolated (see text). Relative intensities are corrected for detection efficiency and internal conversion.

E_γ (keV)	Transition assignment	Relative intensity (%)
(44 ± 1)	$(2^+ \rightarrow 0^+)$	
(104 ± 1)	$(4^+ \rightarrow 2^+)$	
161 ± 1	$(6^+ \rightarrow 4^+)$	100 ± 30
218 ± 1	$(8^+ \rightarrow 6^+)$	80 ± 20
272 ± 1	$(10^+ \rightarrow 8^+)$	53 ± 12
323 ± 1	$(12^+ \rightarrow 10^+)$	49 ± 11
371 ± 1	$(14^+ \rightarrow 12^+)$	22 ± 8
417 ± 2	$(16^+ \rightarrow 14^+)$	20 ± 7
459 ± 2	$(18^+ \rightarrow 16^+)$	18 ± 7
499 ± 2	$(20^+ \rightarrow 18^+)$	16 ± 7

7. Moment of inertia studies

Systematic study of the moments of inertia in a specific region can be a powerful source of information about the properties of rotating nuclei. Indeed, these moments are rather sensitive to the orbitals near the Fermi surface and the pairing strength. Fig. 6.a shows the kinematic moment of inertia as a function of rotational frequency for ^{256}Rf and three other transfermium nuclei: ^{250}Fm, ^{252}No and ^{254}No. The latter three cases were chosen to do isotopic and isotonic comparisons. The curves drawn correspond to the Harris fit to the low-spin part of the observed transition using Eq. (1). One can observe that the behavior of the moment of inertia of ^{256}Rf is quite similar to that of ^{254}No (also a $N = 152$ isotone), with a difference of absolute value over the full frequency range. The rotational properties of the $N = 150$ isotones (^{250}Fm and ^{252}No) are different and exhibit a faster alignment than the $N = 152$ isotones.
One can question the difference of absolute value between these moments. The pairing correlations are expected to diminish at a deformed shell gap, which leads to a higher value for the moment of inertia. The nucleus ^{250}Fm ($Z = 100$, $N = 150$) has the largest moment of inertia. With two additional protons in the ^{252}No nucleus, the moment of inertia drops. This may be due to the reduced influence of the $Z = 100$ deformed shell gap. The same conclusion can be drawn with ^{254}No which has a larger moment of inertia with two neutrons more than ^{252}No, due to the influence of the $N = 152$ deformed shell gap. If there would be a significant deformed shell gap at $Z = 104$, one could expect a higher moment of inertia for ^{256}Rf as compared to ^{254}No. The absence of such an effect suggests that there is no significant gap for $Z = 104$. The difference of moment of inertia can be explained by the decreasing influence of the $Z = 100$ gap.
Fig. 6.b displays the experimental dynamical moment of inertia (calculated with the formula $\mathcal{J}^{(2)} = 2\hbar/[\omega(I) - \omega(I-2)]$ as a function of the rotational frequency normalized by its Harris

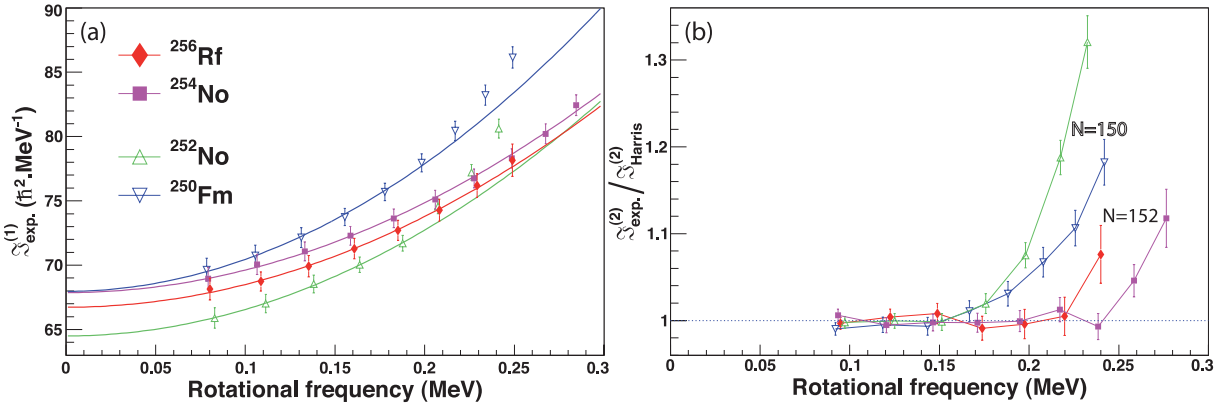

Figure 6. (a) Experimental kinematic moment of inertia as a function of rotational frequency for $N = 150$ and $N = 152$ isotones. The lines correspond to the Harris fits using Eq. (1).
(b) Experimental dynamical moment of inertia as a function of rotational frequency for $N = 150$ and $N = 152$ isotones normalized to the one calculated with the fitted Harris parameters using Eq. (2).

fit using Eq. (2). The same four transfermium nuclei are plotted. At a low rotational frequency the behavior is close to Harris values and experimental values diverge from Harris values for high frequency, a sign of the effect of aligning angular momentum with the rotational axis. This divergence appears at a frequency of 0.15 MeV for the $N = 150$ isotones and at 0.20-0.25 MeV for the $N = 152$ isotones. According to Ref. [23], a competition between neutron $\nu j_{15/2}$ and proton $\pi i_{13/2}$ orbitals in the rotation alignment occurs in these nuclei. The observed differences are due to the relative positions of the relevant orbitals with respect to the Fermi surface. In $N = 150$ isotones, the Fermi surface is just below the neutron $\nu j_{15/2}[734]9/2^-$ orbital and above for $N = 152$ isotones.
Moreover, a delay of the alignment process can be seen between ^{254}No and ^{256}Rf. This effect is due to protons since they are isotones. It is likely to be due to the effect of the proton Fermi surface shift induced by the addition of two protons to ^{254}No driving the $\pi i_{13/2}$ orbital $[624]9/2^+$ closer to the surface for ^{256}Rf.

8. Investigation of Isomeric States

Two recent experiments were dedicated to searches for isomeric states in ^{256}Rf. The first one was performed at the Lawrence Berkeley National Laboratory using the Berkeley Gas-filled Separator [14]. A decay scheme was proposed with three different isomeric multi-quasiparticle states with half-lives of 25 $\pm$ 2, 17 $\pm$ 2 and 27 $\pm$ 5 μs, respectively. A single 900 keV γ-ray decay transition was also observed and interpreted as a decay to ground state band of a low lying $K^\pi=2^-$ structure fed by these isomers. The second experiment was performed at the Argonne National Laboratory using the Fragment Mass Analyzer [15]. A 17 $\pm$ 5 μs isomer was identified with a quite low population and assigned as a 4-qp isomeric state. Thus, both these experiments saw evidence for isomeric states but their conclusions are somewhat contradictory.
In the present experiment, a search for isomeric states in ^{256}Rf was also made using the GREAT focal plane detection system. Since our experiment was dedicated to prompt spectroscopy, the beam intensity was limited and the statistics obtained lower than in previous experiments. The data obtained in the present study and their interpretation are still under analysis and will be published in due course [24].

9. Conclusion

The rotational structure of the superheavy element ^{256}Rf was studied for the first time using state-of-the-art γ-ray spectroscopic techniques. This success took several years as it required the development of a rotating target, the improvement of the γ-ray detector array as well as its electronics. The intense isotopically enriched ^{50}Ti beam development allowed a sufficiently high intensity to be reached to perform the experiment. The systematic study of the moments of inertia of several transfermium nuclei suggests evidence for the effect of weakened pairing correlations due to the presence of deformed shell gaps. The difference of behavior and alignment properties between the isotopes $N = 150$ and $N = 152$ are evidence of the relative proximity to the Fermi surface of the neutron $j_{15/2}$ and proton $i_{13/2}$ orbitals. The observations also suggest the absence of a significant shell gap at $Z = 104$.

Acknowledgments

The authors address special thanks to R. Seppälä, J. Ärje, H. Koivisto, the University of Jyväskylä K130 cyclotron accelerator team and the cyclotron operators. The authors also address special thanks to A. Lecointre from the Department of Analytic Sciences, A. Ouadi, S. Georg, C. Galindo from the Nuclear Chemistry group and the Mechanical Department for all the developments done for the project at IPHC.
This work has been supported by the EU-FP7-IA project ENSAR (No. 262010), the Academy of Finland (CoE in Nuclear ad Accelerator Based Physics, Grant to T.G contract No. 131665), the European Research Council through the project SHESTRUCT (Grant Agreement No. 203481), EURONS (European Commission Contract No. 506065), the UK STFC, the Slovak Grant Agency VEGA (Contract No. 2/0105/11) and the U.S. Department of Energy, Office of Nuclear Physics, under Contract No. DEAC02-06CH11357. The GAMMAPOOL European Spectroscopy Resource is thanked for the loan of detectors for JUROGAM II.

References

[1] Belozerov A V et al. 2003 *Eur. Phys. J. A* **16** 447
[2] Herzberg R D and Greenlees P T 2008 *Prog. Par. Nucl. Phys.* **61** 674
[3] Herzberg R D and Cox D M 2011 *Radiochim. Acta* **99** 441
[4] Bender M et al. 1999 *Phys. Rev. C* **60** 034304
[5] Piot J et al. 2012 *Phys. Rev. C* **85** 041301
[6] Dragojević I et al. 2008 *Phys. Rev. C* **78** 024605
[7] Arnold L et al. 2006 *IEEE Trans. Nucl. Sci.* **53** 723
[8] Piot J et al. *to be published*
[9] Rubert J et al. 2012 *Nucl. Instr. Meth. Phys. Res. B* **276** 33
[10] Lazarus I et al. 2001 *IEEE Trans. Nucl. Sci.* **48** 567
[11] Rahkila P 2008 *Nucl. Instr. Meth. Phys. Res. A* **595** 637
[12] Gall B J P et al. 2011 *Talk at TAN 2011* - http//tan11.jinr.ru/pdf/10_Sep/S_1/04_Gall.pdf
[13] Greenlees P T et al. 2012 *Phys. Rev. Lett.* **109** 012501
[14] Jeppesen H B et al. *Phys. Rev. C* **79** 031303(R)
[15] Robinson A P et al. 2011 *Phys. Rev. C* **83** 064311
[16] Koivisto H et al. 2001 *Nucl. Instr. Meth. Phys. Res. B* **174** 379
[17] Koivisto H et al. 1994 *Nucl. Instr. Meth. Phys. Res. B* **94** 291
[18] Koivisto H et al. 2002 *Nucl. Instr. Meth. Phys. Res. B* **187** 111
[19] Leino M et al. 1995 *Nucl. Instr. Meth. Phys. Res. B* **99** 653
[20] Page R D et al. 2003 *Nucl. Instr. Meth. Phys. Res. B* **204** 634
[21] Hessberger F P et al. 1997 *Z. Phys. A* **359** 315
[22] Harris S 1965 *Phys. Rev.* **138** B509
[23] Bender M et al. 2001 *Nucl. Phys. A* **723** 354
[24] Rubert J et al. *to be published*